0026-895X/09/7602-327–341$20.00
MOLECULAR PHARMACOLOGY
Vol. 76, No. 2
56309/3500015
Mol Pharmacol 76:327–341, 2009
Printed in U.S.A.

BCL-2 Family Inhibitors Enhance Histone Deacetylase Inhibitor and Sorafenib Lethality via Autophagy and Overcome Blockade of the Extrinsic Pathway to Facilitate Killing[S]

Aditi Pandya Martin, Margaret A. Park, Clint Mitchell, Teneille Walker, Mohamed Rahmani, Andrew Thorburn, Dieter Häussinger, Roland Reinehr, Steven Grant, and Paul Dent

Departments of Biochemistry (A.P.M., M.A.P., C.M., T.W., S.G., P.D.) and Medicine (M.R., S.G.) and Institute for Molecular Medicine (S.G., P.D.), Virginia Commonwealth University, Richmond, Virginia; Clinic for Gastroenterology, Hepatology and Infectiology, Heinrich-Heine-University Düsseldorf, Düsseldorf, Germany (D.H., R.R.); and Department of Pharmacology, School of Medicine, University of Colorado Denver, Aurora, Colorado (A.T.)

Received March 18, 2009; accepted May 29, 2009

ABSTRACT

We examined whether the multikinase inhibitor sorafenib and histone deacetylase inhibitors (HDACI) interact to kill pancreatic carcinoma cells and determined the impact of inhibiting BCL-2 family function on sorafenib and HDACI lethality. The lethality of sorafenib was enhanced in pancreatic tumor cells in a synergistic fashion by pharmacologically achievable concentrations of the HDACIs vorinostat or sodium valproate. Overexpression of cellular FLICE-like inhibitory protein (c-FLIP-s) or knockdown of CD95 suppressed the lethality of the sorafenib/HDACI combination (sorafenib + HDACI). In immunohistochemical analyses or using expression of fluorescence-tagged proteins, treatment with sorafenib and vorinostat together (sorafenib + vorinostat) promoted colocalization of CD95 with caspase 8 and CD95 association with the endoplasmic reticulum markers calnexin, ATG5, and Grp78/BiP. In cells lacking CD95 expression or in cells expressing c-FLIP-s, the lethality of sorafenib + HDACI exposure was abolished and was restored when cells were coexposed to BCL-2 family inhibitors [ethyl [2-amino-6-bromo-4-(1-cyano-2-ethoxy-2-oxoethyl)]-4*H*-chromene-3-carboxylate (HA14-1), obatoclax (GX15-070)]. Knockdown of BCL-2, BCL-XL, and MCL-1 recapitulated the effects of GX15-070 treatment. Knockdown of BAX and BAK modestly reduced sorafenib + HDACI lethality but abolished the effects of GX15-070 treatment. Sorafenib + HDACI exposure generated a CD95- and Beclin1-dependent protective form of autophagy, whereas GX15-070 treatment generated a Beclin1-dependent toxic form of autophagy. The potentiation of sorafenib + HDACI killing by GX15-070 was suppressed by knockdown of Beclin1 or of BAX + BAK. Our data demonstrate that pancreatic tumor cells are susceptible to sorafenib + HDACI lethality and that in tumor cells unable to signal death from CD95, use of a BCL-2 family antagonist facilitates sorafenib + HDACI killing via autophagy and the intrinsic pathway.

In the United States, pancreatic carcinomas have 5-year survival rates of less than 5% (Bardeesy and DePinho, 2002; Parkin et al., 2005). This statistic emphasizes the need to develop original therapies using novel targeted agents against this lethal malignancy.

Tumor cells use a wide variety of mechanisms to maintain cell viability, including loss of death receptor expression (e.g., CD95) by reducing expression of proapoptotic BH3 domain proteins (e.g., BAX) or by increasing expression of antiapoptotic BCL-2 family members (e.g., MCL-1) (Lessene et al.,

This work was funded by the National Institutes of Health National Institute of Diabetes and Digestive and Kidney Diseases [Grant R01-DK52825]; the National Institutes of Health National Cancer Institute [Grants P01-CA104177, R01-CA108520, R01-CA63753, R01-CA77141; R01-CA93738]; by The Jimmy V Foundation; and by The Goodwin Foundation for Cancer Research (to Massey Cancer Center). P.D. is the holder of the Universal Inc. Professorship in Signal Transduction Research.

A.P.M., M.A.P., and C.M. contributed equally to this work.

Article, publication date, and citation information can be found at http://molpharm.aspetjournals.org.

doi:10.1124/mol.109.056309.

[S] The online version of this article (available at http://molpharm.aspetjournals.org) contains supplemental material.

ABBREVIATIONS: MEK, mitogen-activated extracellular-regulated kinase; ERK, extracellular regulated kinase; MAPK, mitogen-activated protein kinase; JNK, c-Jun NH_2-terminal kinase; c-FLIP-s, cellular FLICE-like inhibitory protein; ER, endoplasmic reticulum; dn, dominant negative; ca, constitutively active; PERK, PKR-like endoplasmic reticulum kinase; PKR, protein kinase regulated by RNA; HDACI, histone deacetylase inhibitor; GX15-070; HA14-1; TUNEL, terminal deoxynucleotidyl transferase dUTP nick-end labeling; GFP, green fluorescent protein; YFP, yellow fluorescent protein; DMSO, dimethyl sulfoxide; PAGE, polyacrylamide gel electrophoresis; FITC, fluorescein isothiocyanate; PE, phycoerythrin; CMV, cytomegalovirus; siRNA, small interfering RNA; siSCR, scrambled siRNA; DISC, death-inducing signal complex; FADD, FAS-associated death domain; IHC, immunohistochemistry; MEF, mouse embryonic fibroblast.

2008; Kang and Reynolds, 2009; Susnow et al., 2009). In the case of protective BCL-2 family proteins, several clinically relevant small molecule inhibitors have been developed that specifically bind to the BCL-2 family protein, without altering expression of the protein, and block the binding of proapoptotic BH3 domain proteins [e.g., ABT-737 (Oltersdorf et al., 2005); GX15-070] (Zhang et al., 2007; Azmi and Mohammad, 2009). The dissociation of protective BCL-2 proteins from toxic BH3 domain proteins results in greater levels of free BH3 domain protein that will facilitate mitochondrial dysfunction, promote pore formation with alterations in mitochondrial permeability, and facilitate the lethality of other therapeutic agents (Chen et al., 2007; Dai and Grant, 2007).

The apoptotic threshold in tumor cells is also controlled by the activities of multiple signal transduction pathways. The Raf-MEK1/2-ERK1/2 pathway is frequently dysregulated in neoplastic transformation and, along with the MEK5-ERK5, c-Jun NH_2-terminal kinase (JNK1/2) and p38 MAPK pathways, is a member of the MAPK superfamily (Dent et al., 2003, 2009; Dent, 2005; Valerie et al., 2007). These protein kinases are involved in responses to diverse mitogens and environmental stresses and have also been implicated in cell survival processes; activation of the ERK1/2 pathway is associated with survival and JNK1/2 and p38 MAPK pathway signaling with apoptosis. A number of antiapoptotic effector proteins have been identified downstream of ERK1/2 signaling, including increased expression of antiapoptotic proteins such as c-FLIP-s, as well as protective BCL-2 family proteins such as BCL-XL and MCL-1 (Allan et al., 2003; Ley et al., 2003; Mori et al., 2003; Qiao et al., 2003; Grant and Dent, 2004; Wang et al., 2007). In view of the importance of the ERK1/2 pathway in tumor cell growth and survival, inhibitors have been developed that have entered clinical trials, including sorafenib (Bay 43-9006; Nexavar, a Raf kinase inhibitor) and a MEK1/2 inhibitor (Davies et al., 2007; Li et al., 2007).

Sorafenib is a multikinase inhibitor that was originally developed as an inhibitor of Raf-1 but was subsequently shown to inhibit multiple other kinases, including class III tyrosine kinase receptors such as platelet-derived growth factor, vascular endothelial growth factor receptors 1 and 2, c-Kit, and FLT3 (Flaherty, 2007). Some of the antitumor effects of sorafenib have been ascribed to antiangiogenic actions of this agent through inhibition of the growth factor receptors (Gollob, 2005; Strumberg, 2005; Rini, 2006). Several groups have shown in vitro that sorafenib kills human leukemia cells at concentrations below the maximum achievable dose (C_{max}) of 15 to 20 μM, through a mechanism involving down-regulation of the antiapoptotic BCL-2 family member MCL-1 (Rahmani et al., 2005, 2007a). In these studies, sorafenib-mediated MCL-1 down-regulation occurred through a translational rather than a transcriptional or posttranslational process that was mediated by endoplasmic reticulum (ER) stress signaling through PKR-like endoplasmic reticulum kinase (PERK) (Dasmahapatra et al., 2007; Rahmani et al., 2007b).

Histone deacetylase inhibitors (HDACI) represent a class of agents that act by blocking histone deacetylation, thereby modifying chromatin structure and gene transcription. Histone deacetylases, along with histone acetyltransferases, reciprocally regulate the acetylation status of the positively charged NH_2-terminal histone tails of nucleosomes. HDACIs promote histone acetylation and neutralization of positively charged lysine residues on histone tails, allowing chromatin to assume a more open conformation, which favors transcription (Gregory et al., 2001). However, HDACIs also induce acetylation of other nonhistone targets, actions that may have pleiotropic biological consequences, including inhibition of 90-kDa heat shock protein function, induction of oxidative injury, and in some systems up-regulation of death receptor expression (Kwon et al., 2002; Marks et al., 2003; Bali et al., 2005). With respect to combinatorial drug studies with a multikinase inhibitor such as sorafenib, HDACIs are of interest in that they have potential to down-regulate multiple oncogenic kinases by interfering with 90-kDa heat shock protein function, leading to proteasomal degradation of these proteins.

We recently demonstrated that sorafenib synergized with vorinostat to kill liver and kidney cancer cells in a CD95-dependent fashion (Park et al., 2008a; Zhang et al., 2008). Our data also suggested that proteins involved in ER stress signaling coimmunoprecipitated with activated CD95 in hepatoma cells and played a regulatory role in cell survival. The present studies determined whether similar mechanisms of drug action apply in pancreatic tumor cells and whether, in liver and pancreatic tumor cells, restriction or lack of death receptor signaling that blocks lethality induced by the combination of sorafenib and HDACI (sorafenib + HDACI) can be subverted by use of BCL-2 family antagonists.

Materials and Methods

Materials

Sorafenib tosylate was generously provided by Bayer Corp., Pharmaceutical Div. (West Haven, CT) and the National Cancer Institute (Bethesda, MD). Vorinostat was generously provided by Merck (Darmstadt, Germany) and the National Cancer Institute. GX15-070 was generously provided by Gemin X Pharmaceuticals (Malvern, PA) and the National Cancer Institute. The BCL-2/BCL-XL inhibitor HA14-1 was purchased from Calbiochem (San Diego, CA). Phospho-/total- (ERK1/2; JNK1/2; p38 MAPK) antibodies, phospho-/total-AKT (Thr308; Ser473), and the total and cleaved caspase 3 antibodies were purchased from Cell Signaling Technology (Danvers, MA). Anti-BID antibodies were purchased from Cell Signaling Technology. All the secondary antibodies were purchased from Santa Cruz Biotechnology (Santa Cruz, CA). TUNEL kits were purchased from PerkinElmer Life and Analytical Sciences (Waltham, MA) and Boehringer Mannheim (Mannheim, Germany). Trypsin-EDTA, Dulbecco's modified Eagle's medium, RPMI 1640 medium, and penicillin-streptomycin were purchased from Invitrogen (Carlsbad, CA). HEPG2, HEP3B, and HuH7 hepatoma cells and ASPC-3, MiaPaCa2, and PANC1 pancreatic cells were purchased from the American Type Culture Collection (Manassas, VA). BAX(−/−), BAK(−/−), and BAX+BAK(−/−) fibroblasts were kindly provided by Dr. S. Korsmeyer (Harvard University, Boston, MA). Commercially available validated short hairpin RNA molecules to knockdown RNA/protein levels were from QIAGEN (Valencia, CA): CD95 (Hs_FAS_7 HP validated siRNA; Hs_FAS_10 HP siRNA); ATG5 (Hs_APG5L_6 HP validated siRNA); Beclin 1 (Hs_BECN1_1 HP siRNA, Hs_BECN1_3 HP siRNA); BAX (Hs_BAX_10 HP validated siRNA; Hs_BAX_7 HP validated

siRNA); BAK (Hs_BAK1_5 HP validated siRNA; Hs_BAK1_7 HP Validated siRNA). We also used, for confirmatory purposes, the short hairpin RNA construct targeting *ATG5* (pLVTHM/Atg5) that was a gift from Dr. S. Yousefi, (Department of Pharmacology, University of Bern, Switzerland). The plasmids to express green fluorescent protein (GFP)-tagged human LC3; wild-type and dominant-negative PERK (Myc-tagged PERKΔC); yellow florescent protein (YFP)-tagged CD95; and GFP-tagged FAS-associated death domain (FADD) were kindly provided by Dr. S. Spiegel (Virginia Commonwealth University, Richmond, VA), Dr. J. A. Diehl (University of Pennsylvania, Philadelphia, PA), and authors R.R. and A.T., respectively. Reagents and performance of experimental procedures were described previously (Qiao et al., 2001; Dasmahapatra et al., 2007; Mitchell et al., 2007; Rahmani et al., 2007b; Park et al., 2008a,b,c; Yacoub et al., 2008; Zhang et al., 2008).

Methods

Culture and In Vitro Exposure of Cells to Drugs. All established cell lines (HEPG2, HEP3B, and HuH7 hepatoma cells; ASPC-3, MiaPaCa2, and PANC1 pancreatic cells; and wild type, BAX(−/−), BAK −/−, and BAX+BAK(−/−) transformed mouse embryonic fibroblasts) were cultured at 37°C [5% (v/v) CO_2] in vitro using RPMI 1640 medium supplemented with 5% (v/v) fetal calf serum and 10% (v/v) nonessential amino acids. For short-term cell killing assays, immunoblotting and cytochrome *c* release/BH3 domain protein activation studies, cells were plated at a density of 3×10^3 per cm^2 (~2×10^5 cells per well of a 12-well plate); 48 h after plating, cells were treated with various drugs. Hepatoma cells were treated with 3 μM sorafenib, 500 nM vorinostat, or 1 mM sodium valproate unless otherwise indicated. Pancreatic cancer cells were treated with 6 μM sorafenib, 500 nM vorinostat, or 1 mM sodium valproate unless otherwise indicated. Unless otherwise indicated, GX15-070 and HA14-1 treatments were 100 nM and 10 μM, respectively. In vitro vorinostat, sorafenib, and GX15-070 treatments were from 100 mM stock solutions of each drug, and the maximal concentration of vehicle (DMSO) in media was 0.02% (v/v). Sodium valproate was from a stock 1 M solution. Cells were not cultured in reduced serum media during any study in this manuscript.

In Vitro Cell Treatments, Microscopy, SDS-PAGE and Western Blot Analysis. For in vitro analyses of short-term cell death effects, cells plated in triplicate were treated with vehicle, vorinostat, or sodium valproate + sorafenib for the times indicated in the figure legends. For apoptosis assays where indicated, cells were pretreated with vehicle (DMSO) and therapeutic drugs; floating and attached cells were isolated at the indicated times (24–96 h) and subjected to trypan blue cell viability assay by counting in a light microscope. Alternatively, the Annexin V/propidium iodide assay was carried to determine cell viability out according to the manufacturer's instructions (BD Pharmingen, San Diego, CA) using a BD FACScan flow cytometer. Vorinostat or sodium valproate/sorafenib lethality, as judged by annexin-propidium iodide, was first evident ~24 h after drug exposure (data not shown). Data are plotted as either percentage cell death or the true percentage of cell death with the amount of cell killing in vehicle-treated cells subtracted from the total. For microscopy, cells were plated into eight-chambered glass slides and 24 h later treated with drugs. Six hours after drug treatment, cells were fixed and permeabilized. Cells were stained with the indicated primary antibodies (CD95, Grp78/BiP, ATG5, Calnexin) and visualized with secondary antibodies with conjugated fluorescent probes (FITC, PE). Cells were visualized using the appropriate fluorescent light filters at 40×, and images were merged using Photoshop CS2 (Adobe Systems, Mountain View, CA). Areas of protein-protein colocalization appear as yellow/orange.

For SDS PAGE and immunoblotting, cells were plated at 5×10^5 cells/cm^2 and treated with drugs at the indicated concentrations; after the indicated time of treatment, they were lysed in whole-cell lysis buffer (0.5 M Tris-HCl, pH 6.8, 2% SDS, 10% glycerol, 1% β-mercaptoethanol, 0.02% bromphenol blue), and the samples were boiled for 30 min. The boiled samples were loaded onto 10 to 14% SDS-PAGE and electrophoresis was run overnight. Proteins were electrophoretically transferred onto 0.22 μm nitrocellulose and immunoblotted with various primary antibodies against different proteins. Immunoblots were visualized by an Odyssey infra red imaging system. For presentation, immunoblots after scanning were processed using Adobe PhotoShop CS2, and figures were generated in PowerPoint 2007 (Microsoft Corp, Redmond, WA).

Infection of Cells with Recombinant Adenoviruses. Cells were plated at 3×10^3 cells/cm^2 in each well of an eight-chambered glass slide, a 12- or a 6-well plate, or a 60-mm plate. After plating (24 h), cells were infected (hepatoma and pancreatic carcinoma cells at a multiplicity of infection of 50) with a control empty vector virus (CMV) and adenoviruses to express constitutively activated (ca) MEK1 (caMEK1), activated caAKT, dominant-negative (dn) AKT, dnMEK1, the caspase 8 inhibitor CRM A, dominant-negative caspase 9, c-FLIP-s, BCL-XL, or XIAP (Vector Biolabs, Philadelphia, PA). After infection (24 h), cells were treated with the indicated concentrations of vorinostat or sodium valproate/sorafenib and/or other drugs, and cell survival or changes in expression/phosphorylation were determined 0 to 96 h after drug treatment by trypan blue/TUNEL/flow cytometry assays and immunoblotting.

Transfection of Cells with siRNA or with Plasmids. *For plasmids.* Cells were plated as described above and transfected 24 h after platin. For mouse embryonic fibroblasts (2–5 μg) or other cell types (0.5 μg), plasmids expressing a specific mRNA (or siRNA) or appropriate vector control plasmid DNA were diluted in 50 μl of serum- and antibiotic-free medium (1 portion for each sample). Concurrently, 2 μl of Lipofectamine 2000 (Invitrogen) was diluted into 50 μl of serum- and antibiotic-free medium (one portion for each sample). Diluted DNA was added to the diluted Lipofectamine 2000 for each sample and incubated at room temperature for 30 min. This mixture was added to each well or dish of cells containing 200 μl of serum- and antibiotic-free medium for a total volume of 300 μl, and the cells were incubated for 4 h at 37°C. An equal volume of 2× medium was then added to each well. Cells were incubated for 24 h, then treated with vorinostat + sorafenib.

For siRNA. Cells were plated in 60-mm dishes from a fresh culture growing in log phase as described above, and transfected24 h after plating. Before transfection, the medium was aspirated and 1 ml of serum-free medium was added to each plate. For transfection, 10 nM concentrations of the annealed siRNA, the positive sense control double-stranded siRNA targeting GAPDH, or the negative control [a "scrambled" (siSCR) sequence with no significant homology to any known gene sequences from mouse, rat or human cell lines] was used. siRNA (10 nM; scrambled or experimental for knockdown) was diluted in serum-free media. HiPerFect (4 μl; QIAGEN) was added to this mixture, and the solution was mixed by pipetting up and down several times. This solution was incubated at room temp for 10 min then added dropwise to each dish. The medium in each dish was swirled gently to mix and then incubated at 37°C for 2 h. One milliliter of 10% (v/v) serum-containing medium was added to each plate, and cells were incubated at 37°C for 36 h before treatment with vorinostat + sorafenib (0–96 h). Trypan blue exclusion/TUNEL/flow cytometry assays and SDS-PAGE/immunoblotting analyses were performed at the time points indicated in each figure.

Isolation of a Crude Cytosolic Fraction. A crude membrane fraction was prepared from treated cells. In brief, cells were washed twice in ice-cold isotonic HEPES buffer (10 mM HEPES, pH 7.5, 200 mM mannitol, 70 mM sucrose, 1 μM EGTA, 10 μM protease inhibitor cocktail; Sigma, St. Louis, MO). Cells on ice were scraped into isotonic HEPES buffer and lysed by passing 20 times through a 25-gauge needle. Large membrane pieces, organelles, and unlysed cells were removed from the suspension by centrifugation at 120*g* for 5

min. The crude granular fraction and cytosolic fraction was obtained from by centrifugation for 30 min at 10,000*g*, leaving the cytosol as supernatant.

Data Analysis. Comparison of the effects of various treatments was performed using analysis of variance and the Student's *t* test. Differences with a p value of < 0.05 were considered statistically significant. Experiments shown are the means of multiple individual points (± S.E.M.). Median dose effect isobologram analyses to determine synergism of drug interaction were performed according to the methods of T.-C. Chou and P. Talalay using the Calcusyn program for Windows (BIOSOFT, Cambridge, UK). Cells are treated with agents at a fixed concentration dose. A combination index value of less than 1.00 indicates synergy of interaction between the drugs; a value of 1.00 indicates additivity; a value of > 1.00 equates to antagonism of action between the agents.

Results

Vorinostat (suberoylanilide hydroxamic acid; Zolinza) is a hydroxamic acid HDACI that has shown preliminary preclinical evidence of activity in hepatoma and other malignancies with a C_{max} of ~9 μM; however, the agent has a very short half-life in plasma and steady-state drug levels in many patients are ~1 μM or less (Pang and Poon, 2007; Venturelli et al., 2007; Wise et al., 2007). Treatment of pancreatic tumor cells (PANC1, MiaPaca2, ASPC-1) with concentrations of vorinostat and sorafenib that are sustainable in patient serum resulted in a greater than additive increase in tumor cell killing as assessed by short-term death assays (nuclear fragmentation by 4,6-diamidino-2-phenylindole stain; trypan blue exclusion) and a synergistic increase in killing assessed by colony formation assays performed using median dose effect isobologram analyses (Fig. 1, A-C; Tables 1 and 2). Suppression of caspase 8 function, as well as expression of dominant negative caspase 9 or BCL-XL also blunted sorafenib + vorinostat lethality (Fig. 1A). Similar data to those in human tumor cell lines were obtained using the rodent pancreatic tumor line PAN02 (Supplemental Fig. 1).

Sorafenib + vorinostat, but not treatment with the individual drugs, activated CD95 and caused formation of a death-inducing signal complex (DISC) containing caspase 8, FADD, ATG5, and Grp78/BiP (Fig. 1, D and E, and Supplemental Fig. 2). The ability of sorafenib + vorinostat to kill pancreatic tumor cells was suppressed by constitutive expression of c-FLIP-s, by knockdown of CD95, or by expression of dominant-negative PERK (Fig. 1F, Table 1; Supplemental Figs. 2 and 3). Treatment of pancreatic tumor cells with sorafenib + HDACI enhanced phosphorylation of PERK and its substrate eukaryotic translation initiation factor 2α and decreased expression of BID and c-FLIP-s (Supplemental Fig. 3). Sodium valproate is an anticonvulsive drug that also has HDACI activity (Rodriguez-Menendez et al., 2008). A clinically relevant and sustainable concentration of sodium valproate enhanced sorafenib lethality in a synergistic fashion in pancreatic tumor cells derived from either humans or rodents as judged in short-term cell death assays and in median dose effect isobologram colony formation assays (Supplemental Fig. 1 and Table 2).

Sorafenib is an inhibitor of RAF family protein kinases that regulate the ERK1/2 pathway as well as an inhibitor of class III receptor tyrosine kinases that regulate the phosphatidyl inositol 3 kinase-AKT pathway. Hence, we determined whether modulation of ERK1/2 and/or AKT activity altered the lethality of sorafenib + vorinostat exposure. Expression of constitutively activated MEK1 EE suppressed sorafenib + HDACI lethality in pancreatic and liver cancer cells, and in hepatoma cells expression of activated AKT also suppressed drug lethality (Supplemental Fig. 4). Expression of dnMEK1 and dnAKT, but not the individual activated kinase, was required to enhance the lethality of sorafenib + vorinostat exposure. Thus the regulation of sorafenib + HDACI lethality occurs via both the ERK1/2 and AKT pathways in pancreatic and liver cancer cells. The findings in Fig. 1, Tables 1 and 2, and Supplemental Figs. 1 to 4 demonstrate that sorafenib + HDACI exposure induces an endoplasmic reticulum stress response in pancreatic tumor cells that promotes tumor cell death.

CD95 is known to mediate proapoptotic signaling through its association with FADD, and FADD by binding to procaspase 8 promoting auto-catalytic activation of pro-caspase 8, in the DISC. To further examine the biology of CD95 signaling after drug treatment, we performed immunohistochemistry (IHC) in permeabilized cells with confocal microscopic examination for the cellular localization of multiple extrinsic apoptosis pathway/autophagy/ER stress regulatory proteins. In permeabilized HEP3B cells 6 h after sorafenib + vorinostat treatment, we noted by IHC that CD95 colocalized with Grp78/BiP and ATG5 (Fig. 2, A and B, white arrows indicate protein colocalization). We next attempted to confirm our findings using immunoprecipitation and IHC using expression of transfected fluorescent-tagged proteins. Transfection of hepatoma cells with plasmids to express CD95-YFP in combination with a construct to express ATG5-cherry red or FADD-GFP in combination with a construct to express ATG5-cherry red demonstrated within 6 h after drug exposure that CD95 became visibly punctate and, based on the merging of images from the confocal microscope, that CD95 became associated with both ATG5 and FADD (Fig. 2, C and D). In permeabilized HEP3B cells 6 h after sorafenib + vorinostat treatment, we noted by IHC that CD95 colocalized with the ER associated protein calnexin (Fig. 2E). Collectively, our findings argue that sorafenib and HDACI treatment rapidly promote activation of CD95 at internal sites within a tumor cell and that "activated" CD95 subsequently migrates to the plasma membrane.

Based on data showing that knockdown of CD95 expression reduced sorafenib + vorinostat lethality, we next explored whether cells lacking CD95 were resistant to drug-induced killing and whether re-expression of CD95 enhanced drug lethality. HuH7 cells that lack CD95 expression were relatively resistant to the lethal effects of sorafenib + vorinostat exposure (Fig. 3, A and B). Transient re-expression of CD95 in HuH7, with a CD95-YFP construct, significantly enhanced sorafenib + vorinostat lethality (Fig. 3C). We demonstrated previously that overexpression of the BCL-2 family protein BCL-XL suppressed sorafenib + vorinostat-induced killing (Zhang et al., 2008). Using transformed mouse embryonic fibroblasts in which specific toxic BH3 domain proteins were deleted, we also found that loss of BAX and BAK expression profoundly reduced the toxic interaction between sorafenib + vorinostat and also between sorafenib and sodium valproate (Supplemental Fig. 5). Based on these findings, we then explored whether drugs that block the interaction of toxic BH3 domain proteins with protective BCL-2 family members could enhance the lethality of sorafenib +

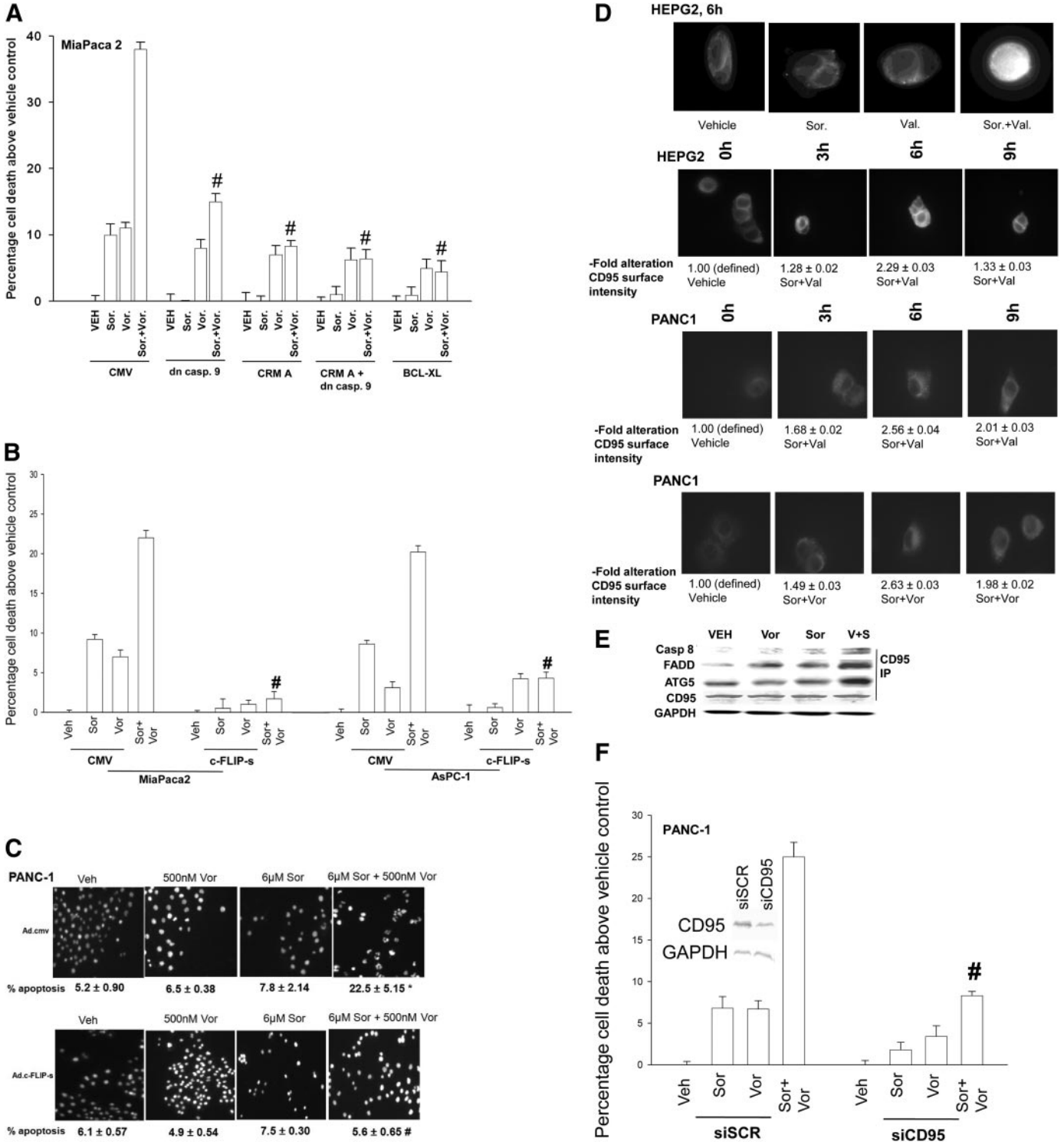

Fig. 1. Sorafenib and vorinostat interact in a synergistic fashion to kill pancreatic cancer cells via the death receptor CD95. A, MiaPaca2 cells were infected with the indicated recombinant adenoviruses. Cells were treated with vehicle, sorafenib, vorinostat or sorafenib + vorinostat as described under *Materials and Methods*. Cells were isolated after 96 h, and viability was determined by trypan blue assay ($n = 3$, ± S.E.M.) # $p < 0.05$ less cell killing than compared with parallel condition in vehicle treatment cells. B and C, MiaPaca2, PANC1, and AsPC1 cells were infected with the indicated recombinant adenoviruses and subsequently treated with vehicle, sorafenib, vorinostat or sorafenib + vorinostat. Cells were isolated 48 h later and viability determined using MiaPaca2 and AsPC1 cells in trypan blue exclusion (± S.E.M., $n = 3$). #, $p < 0.05$ less than corresponding value in CMV vector cells; PANC1 cells, 4,6-diamidino-2-phenylindole to examine nuclear morphology. Pictorial data are from a representative study ($n = 3$, ± S.E.M.). ∗, $p < 0.01$ greater than vehicle control; #, $p < 0.01$ less than corresponding value in CMV-infected cells. D, HEPG2 and PANC1 cells were treated with vehicle, vorinostat, sodium valproate, sorafenib, sorafenib + vorinostat, or sorafenib + valproate. After treatment (6 h), cells were fixed but not permeabilized. Cells were stained with anti-CD95 antibody and visualized with a FITC secondary antibody at 40× magnification. Data are a representative study (± S.E.M. $n = 3$ for CD95 quantitation). E, PANC1 cells were treated with vehicle, vorinostat, sorafenib, or sorafenib + vorinostat. Six hours after exposure, cells were lysed and CD95 was immunoprecipitated to determine the presence of indicated associated proteins in the DISC. F, PANC-1 cells were transfected with siRNA molecules and subsequently treated with vehicle, vorinostat, sorafenib, or sorafenib + vorinostat. Forty-eight hours after drug exposure, cell viability was determined using a trypan blue exclusion assay (± S.E.M., $n = 3$). #, $p < 0.05$ less than corresponding value in CMV vector cells.

HDACI treatment, and whether inhibitors of cytoprotective BCL-2 family proteins could restore drug-induced killing in a CD95-null/knocked down environment. This is of potential clinical importance because CD95 expression and functional signaling by this death receptor is often lost in the more advanced metastatic tumors.

Treatment of HEPG2 or HEP3B cells with a low concentration of the BCL-2 and BCL-XL antagonist HA14-1 significantly enhanced the lethal effects of the primary sorafenib + vorinostat treatment (Fig. 3D). In HEPG2 cells expressing c-FLIP-s, the lethality of sorafenib + vorinostat treatment was abolished; however, in the presence of HA14-1, a significant large portion of primary sorafenib + vorinostat-induced killing was regained regardless of c-FLIP-s levels (Fig. 3E). This correlated with restoration of drug-induced cytochrome *c* release into the cytosol (Fig. 3F). Furthermore, in CD95-null HuH7 cells, HA14-1 coexposure significantly enhanced sorafenib + vorinostat lethality (Fig. 3G). The relative increase in cell killing caused by sorafenib + vorinostat ± HA14-1 exposure was also reflected in the enhanced release of cytochrome *c* from the mitochondria into the cytosolic fraction (Fig. 3H). The findings in HuH7 cells, which lack endogenous CD95 protein expression, suggest that even in the absence of CD95, disruption of BCL-2 family protective mechanisms facilitates sorafenib + vorinostat lethality.

TABLE 1

Sorafenib synergizes with vorinostat to kill pancreatic tumor cells that is abolished by overexpression of c-FLIP-s

Pancreatic cancer (Mia Paca 2, PANC1, AsPc1) and hepatoma (HEP3B) cells were infected 12 h after plating at an approximate multiplicity of infection of 50 with either a control empty vector recombinant adenovirus (CMV) or a recombinant virus to express the caspase 8 inhibitor c-FLIP-s. Twenty-four hours after infection, infected cells were plated as single cells (250–1500 cells/well) in sextuplicate; 12 h after this plating, the infected cells were treated with vehicle (DMSO), sorafenib (3.0–6.0 μM), vorinostat (250–500 nM), or both drugs combined, as indicated, at a fixed concentration ratio to perform median dose-effect analyses for the determination of synergy. After drug exposure (48 h), the medium was changed, and cells were cultured in drug-free medium for an additional 10 to 14 days. Cells were fixed and stained with crystal violet, and colonies of >50 cells/colony were counted. Colony formation data were entered into the Calcusyn program, and combination index (CI) values were determined. A CI value of less than 1.00 indicates synergy.

Cell Lines & Treatments	Sorafenib	Vorinostat	Fa	CI
	μM	μM		
Mia Paca2				
CMV	3.00	0.250	0.34	0.32
	4.50	0.375	0.42	0.40
	6.00	0.500	0.50	0.45
c-FLIP-s	3.00	0.250	0.16	0.98
	4.50	0.375	0.21	1.23
	6.00	0.500	0.26	1.42
PANC1				
CMV	3.00	0.250	0.22	0.38
	4.50	0.375	0.28	0.42
	6.00	0.500	0.36	0.38
c-FLIP-s	3.00	0.250	0.06	0.92
	4.50	0.375	0.10	1.00
	6.00	0.500	0.16	1.03
AsPc1				
CMV	3.00	0.250	0.34	0.34
	4.50	0.375	0.48	0.40
	6.00	0.500	0.58	0.45
c-FLIP-s	3.00	0.250	0.06	1.08
	4.50	0.375	0.11	0.96
	6.00	0.500	0.19	0.77
Hep3B				
CMV	3.00	0.250	0.43	0.47
	4.50	0.375	0.56	0.58
	6.00	0.500	0.74	0.58
c-FLIP-s	3.00	0.250	0.26	0.90
	4.50	0.375	0.40	0.97
	6.00	0.500	0.54	1.08

We next determined whether a more clinically relevant BCL-2 family inhibitor, GX15-070 (obatoclax), which inhibits BCL-2, BCL-XL, *and* MCL-1 function and is entering phase II trials, could promote sorafenib + HDACI killing. A 48-h exposure of HEPG2 cells to 1 and 3 μM sorafenib resulted in modest increases in cell killing that became larger in cells exposed to 6 and 10 μM sorafenib (Fig. 4A). GX15-070 treatment in the clinically relevant 50 to 250 nM dose range caused similar amounts of cell death in short-term viability assays regardless of dose, approximately 7 to 10% above vehicle control levels. We noted that GX15-070 treatment abolished the modest levels of sorafenib-induced cell death in the 1 to 3 μM dose range and blunted the lethality of higher dose sorafenib with an interaction that was less than additive (Fig. 4A). GX15-070 treatment did not significantly enhance as single agents the amount of cell killing caused by the HDACIs vorinostat or sodium valproate in our cell system (Fig. 4B). However, GX15-070 treatment significantly enhanced the level of killing caused by sorafenib + valproate exposure (Fig. 4, C and D). GX15-070 as a single agent activated BAX and did not seem to further enhance sorafenib + valproate-induced BAX activation (Fig. 4E). GX15-070 as a single agent also activated BAK, and interacted in at least an additive fashion with sorafenib + valproate treatment to cause further BAK activation. In a manner similar to that of sorafenib + vorinostat exposure, these findings also correlated with sorafenib + valproate-inducing decreased expression of protective BCL-2 family proteins (Fig. 4F). Unlike sorafenib + valproate treatment, GX15-070 as a single agent did not alter BCL-2 family protein expression and did not appear to further reduce BCL-2 family protein expression in the presence of sorafenib + HDACI (data not shown).

We next determined, in a manner similar to that used for HA14-1, whether GX15-070 could restore drug-induced lethality in a cellular environment lacking CD95 death receptor signaling. The lethality of sorafenib + valproate exposure was blocked by overexpression of c-FLIP-s or knockdown of CD95 in short-term viability assays (Fig. 5, A and B). GX15-070 enhanced sorafenib + valproate lethality and abolished the protective effect caused by either overexpression of

TABLE 2

Sorafenib synergizes with sodium valproate to kill pancreatic and liver tumor cells.

Pancreatic cancer (Mia Paca2, PANC1) and hepatoma (HEP3B) cells 12 h after plating were treated with vehicle (DMSO), sorafenib (2.25–9.00 μM), sodium valproate (0.50–1.50 mM), or with both drugs combined, as indicated, at a fixed concentration ratio to perform median dose-effect analyses for the determination of synergy. After drug exposure (48 h), the medium was changed, and cells cultured in drug-free medium for an additional 10 to 14 days. Cells were fixed, and stained with crystal violet, and colonies of >50 cells/colony were counted. Colony formation data were entered into the Calcusyn program, and combination index (CI) values were determined. A CI value of less than 1.00 indicates synergy.

Cell Lines	Sorafenib	Valproate	Fa	CI
	μM	mM		
MiaPaca2	2.25	0.75	0.35	0.82
	3.00	1.00	0.46	0.73
	3.75	1.25	0.54	0.65
HEP3B	2.25	0.75	0.17	0.69
	3.00	1.00	0.19	0.68
	3.75	1.25	0.36	0.54
PANC1	3.0	0.50	0.37	0.46
	4.5	0.75	0.43	0.58
	6.0	1.00	0.54	0.57
	7.5	1.25	0.73	0.41
	9.0	1.50	0.80	0.37

c-FLIP-s or knockdown of CD95. This effect was also observed in long-term colony formation assays in PANC-1 cells (Table 3, data not shown). The restoration of drug-induced lethality correlated with restoration of cytochrome *c* release into the cytosol in cells treated with GX15-070 and with sorafenib + HDACI + GX15-070 (Fig. 5C). Enhanced sorafenib + valproate lethality correlated with reduced coimmunoprecipitation of toxic BH3 domain proteins with MCL-1 (Fig. 5D). Of particular note, BAK association with MCL-1 was reduced within 6 h of drug exposure, before any reduction in BCL-2 family protein levels, that correlated with activation of CD95/caspase 8 and loss of full-length BID expression (Fig. 5D and Supplemental Fig. 3). In parallel to these events, sorafenib + valproate treatment caused increased association of BAK and BAX with mitochondria and a reduction in the levels of these proteins in the cytosol (Fig. 5E). Similar apoptosis and blotting data to that observed in hepatoma cells were also obtained in pancreatic tumor cells (Fig. 6, A and B; data not shown).

GX15-070 is an inhibitor of BCL-2, BCL-XL, and MCL-1 function, whereas HA14-1 is an inhibitor of only BCL-2 and BCL-XL function, and we next determined whether individual or combined molecular knockdown of these BCL-2 family proteins resulted in enhanced sorafenib + valproate lethality (Chen et al., 2007; Nguyen et al., 2007; Konopleva et al., 2008). Knockdown of BCL-2 or BCL-XL or MCL-1 modestly

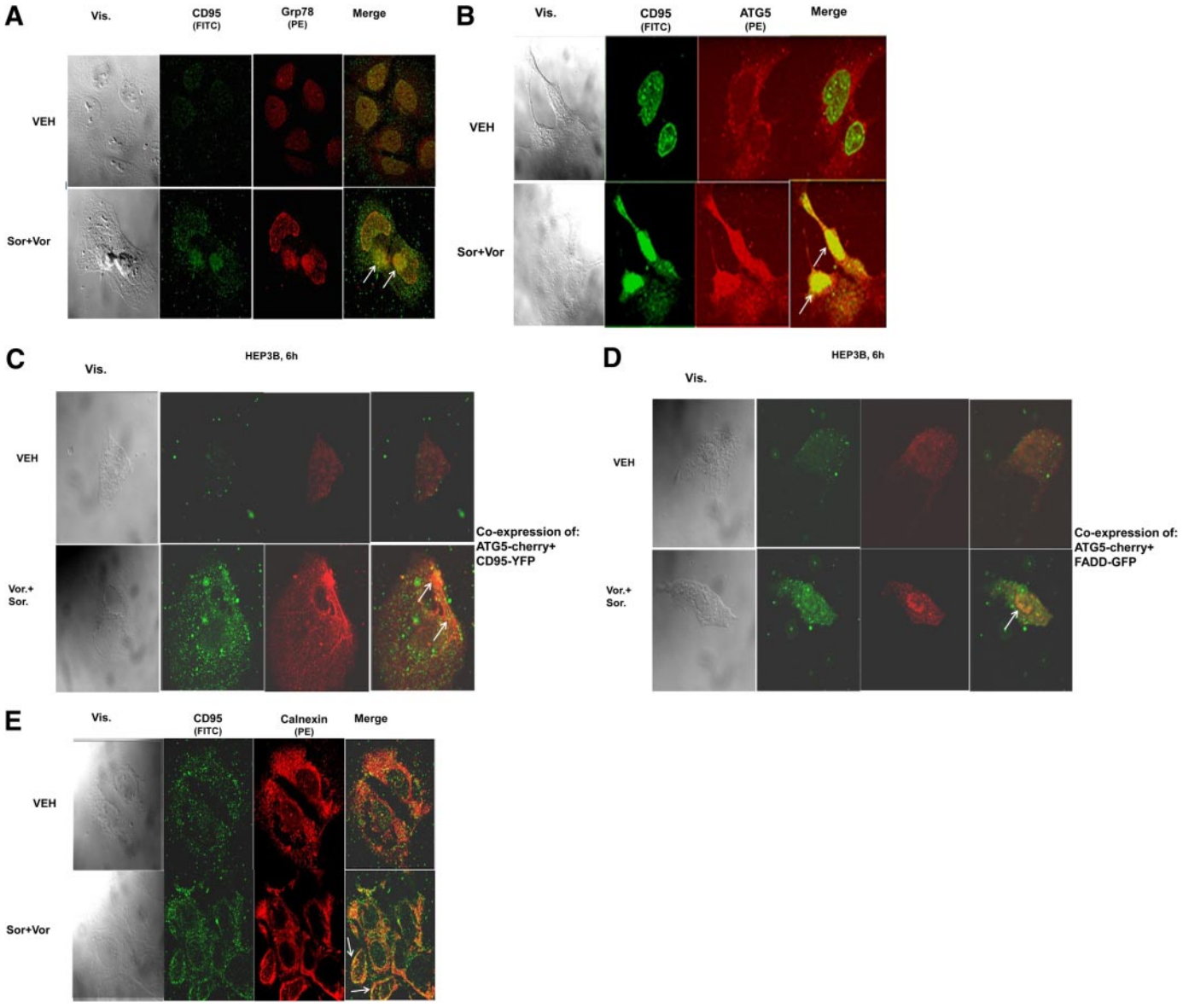

Fig. 2. Sorafenib and HDACIs cause CD95 to associate with ER resident proteins that correlate with CD95 plasma membrane localization and DISC formation. A and B, HEPG2 cells were treated with vehicle, vorinostat, sorafenib, or sorafenib + vorinostat as described under *Materials and Methods*. After drug treatment, cells were fixed, permeabilized, and stained with the indicated primary antibodies and visualized with secondary antibodies with conjugated fluorescent probes (FITC, PE). Data are from a representative study ($n = 3$). C and D, HEP3B cells were transfected as indicated with plasmids and subsequently were treated with vehicle, vorinostat, sorafenib, or sorafenib + vorinostat. Six hours after drug treatment cells were placed onto a confocal microscope stage and using appropriate filters, images of live cells captured at 40× magnification. Data in each are from a representative study ($n = 3$). E, HEPG2 cells were treated with vehicle, vorinostat, sorafenib, or sorafenib + vorinostat. Six hours after drug treatment, cells were fixed and permeabilized. Cells were stained with the indicated primary antibodies and visualized with secondary antibodies with conjugated fluorescent probes (FITC, PE). Cells were visualized using the appropriate fluorescent light filters at 40×. Data are from a representative study ($n = 3$).

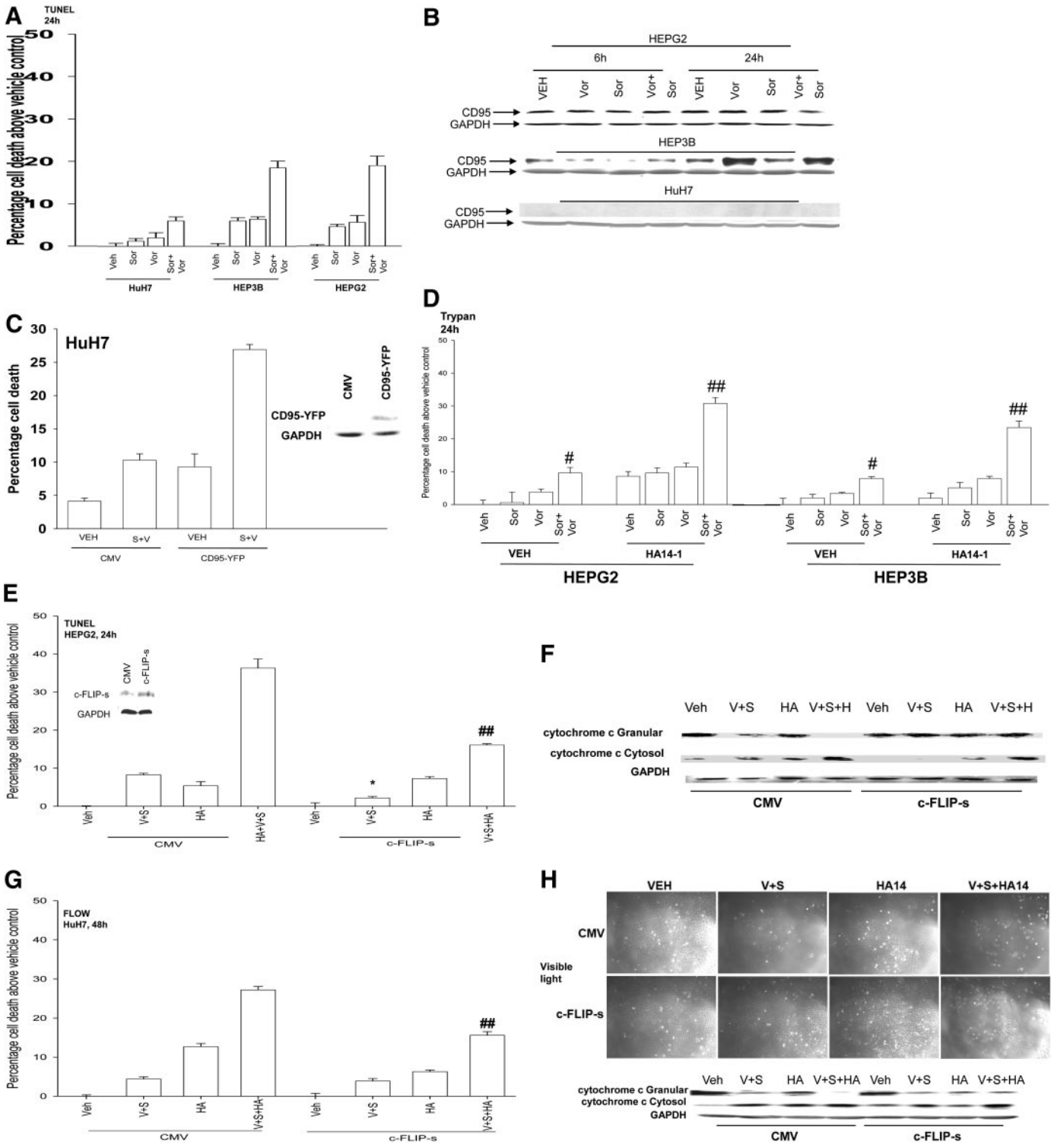

Fig. 3. The BCL-2/BCL-XL inhibitor HA14-1 promotes sorafenib + vorinostat-induced killing and circumvents the protective effects of either CD95 knockdown or c-FLIP-s overexpression. A, HuH7, HEPG2, and HEP3B cells were treated with vehicle, vorinostat, sorafenib, or sorafenib + vorinostat. Forty-eight hours after drug exposure, cell viability was determined using a TUNEL assay for DNA strand breaks (± S.E.M., $n = 3$). B, hepatoma cells were isolated 6 and 24 h after drug exposure, and immunoblotting was performed to determine the expression of CD95 and GAPDH (a representative, $n = 2$–5). C, HuH7 cells 24 h after plating in triplicate were transfected with an empty vector plasmid (CMV) or a plasmid to express CD95-YFP and subsequently were treated with vehicle and sorafenib + vorinostat. Forty-eight hours after drug exposure, cell viability determined by trypan blue exclusion assay (± S.E.M., $n = 2$). D, HEPG2 and HEP3B cells were treated with vehicle, vorinostat, sorafenib, or sorafenib + vorinostat and in parallel with either vehicle or HA14-1. Twenty-four hours after exposure, cell viability was determined using trypan blue exclusion (± S.E.M., $n = 2$). #, $p < 0.05$ greater than vehicle control; ##, $p < 0.05$ greater than cells lacking HA14-1. E, HEPG2 cells were infected with recombinant adenoviruses and were subsequently treated with vehicle, vorinostat, sorafenib, or sorafenib + vorinostat and in parallel with either vehicle (DMSO) or HA14-1. Twenty-four hours after exposure, cell viability was determined using TUNEL assays (± S.E.M., $n = 2$). *, $p < 0.05$ less than corresponding value in CMV vector cells; ##, $p < 0.05$ greater than cells lacking HA14-1. F, sets of infected cells parallel to those in E were treated with drugs, and 24 h after exposure, cell fractionation to isolate the crude granular and cytosolic fractions was performed to determine cytochrome *c* levels ($n = 2$). G, HuH7 cells were infected with recombinant adenoviruses and subsequently treated with vehicle, vorinostat, sorafenib, or sorafenib + vorinostat, and in parallel with either vehicle (DMSO) or HA14-1. Forty eight hours after exposure, cell viability was determined using Annexin V–propidium iodide flow cytometry assays (± S.E.M., $n = 2$). ##, $p < 0.05$ greater than cells lacking HA14-1. H, parallel sets of infected HuH7 cells were treated with drugs, and 24 h after exposure, cell fractionation to isolate the crude granular and cytosolic fractions was performed to determine cytochrome *c* levels ($n = 2$).

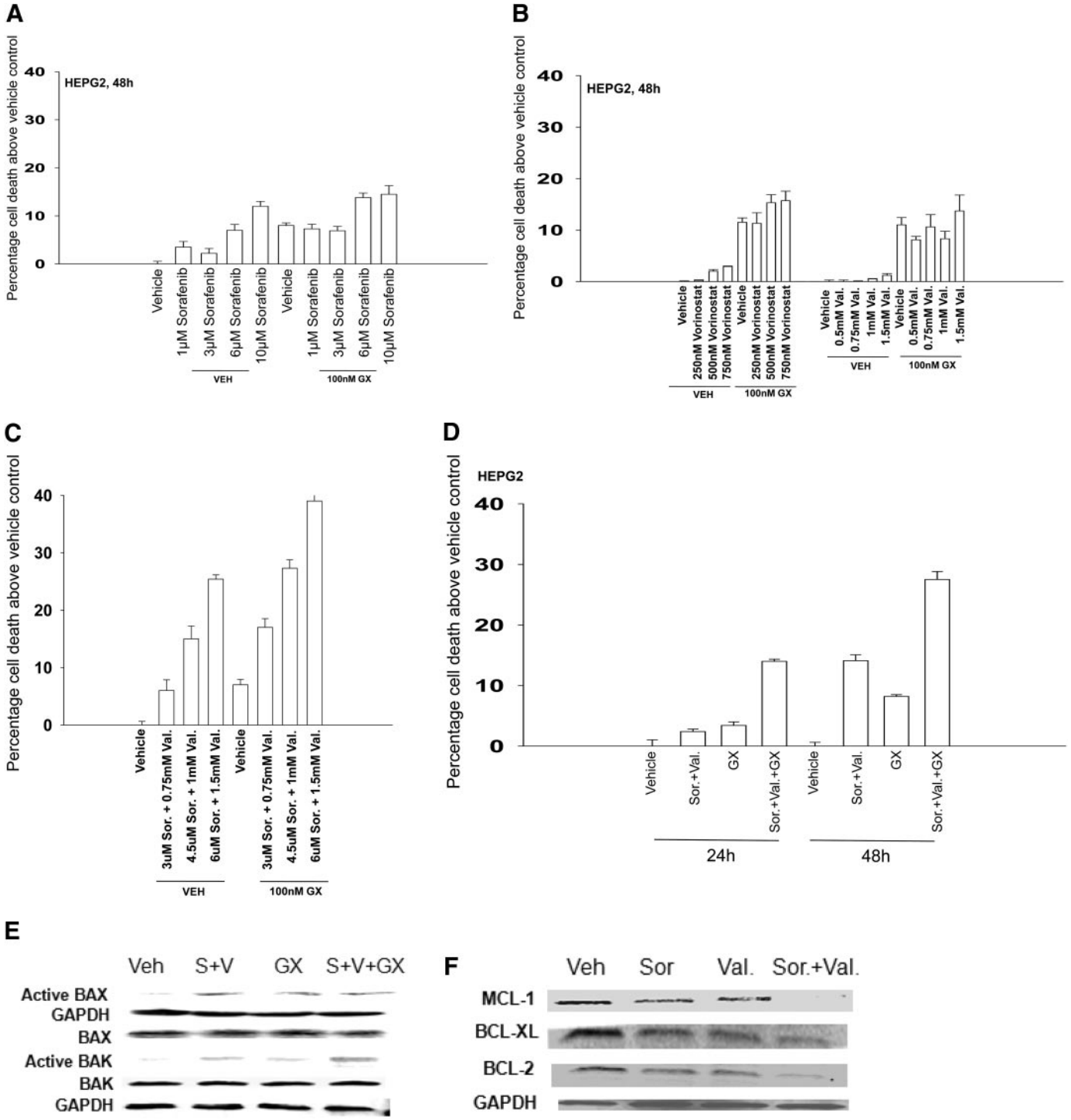

Fig. 4. Sorafenib and sodium valproate combination lethality is enhanced by GX15-070 (obatoclax). A, HEPG2 cells were treated with vehicle or GX15-070 in the presence or absence of sorafenib. Cells were isolated after 48 h, and viability was determined using trypan blue exclusion (± S.E.M., $n = 3$). B, HEPG2 cells were treated with vehicle or GX15-070 in the presence or absence of either vorinostat or sodium valproate. Cells were isolated after 48 h, and viability was determined using trypan blue exclusion (± S.E.M., $n = 3$). C, HEPG2 cells were treated with vehicle or GX15-070 in the presence or absence of sodium valproate and sorafenib. Cells were isolated 48 h after exposure, and viability was determined using trypan blue exclusion (± S.E.M., $n = 3$). D, HEPG2 cells were treated with vehicle or GX15-070 in the presence or absence of sorafenib and sodium valproate. Cells were isolated 24 and 48 h after drug exposure, and viability was determined using trypan blue exclusion (± S.E.M., $n = 3$). E, HEPG2 cells were treated with vehicle or GX15-070 in the presence or absence of sodium valproate and sorafenib. Twenty-four hours after treatment, the activation of BAX and BAK was determined after immunoprecipitation ($n = 3$). F, HEPG2 cells were treated with vehicle in the presence or absence of sodium valproate and/or sorafenib. Twenty-four hours after treatment, the expression of BCL-2, BCL-XL, and MCL-1 was determined by SDS-PAGE/blotting ($n = 3$).

though significantly enhanced sorafenib + valproate lethality (Fig. 6C). Knockdown of BCL-2 and BCL-XL to mimic the actions of HA14-1 or knockdown of BCL-2, BCL-XL, and MCL-1 to mimic the actions of GX15-070 caused significantly greater enhancements of sorafenib + valproate lethality than knockdown of any individual BCL-2 family protein. Based on an additive summation of enhanced cell killing due to individual BCL-2 family protein knockdown, we would have predicted that knockdown of BCL-2 and BCL-XL would have elevated sorafenib + HDACI lethality by an additional 13.5% above control value, whereas in fact, we observed a 23.0% increase above control ($p < 0.05$). We would have predicted that knockdown of BCL-2, BCL-XL, and MCL-1 would have elevated drug lethality by an additional 22.0% based on the additive effect of each individual knockdown, whereas we observed a 31.5% increase ($p < 0.05$). These findings suggest that the major targets of HA14-1/GX15-070 action when combined with sorafenib + valproate are BCL-2/BCL-XL rather than MCL-1. In partial agreement with our data in transformed MEFs and with data in Figs. 4 and 5, combined knockdown of BAX and BAK expression modestly suppressed sorafenib + valproate killing in HEPG2 cells (Fig. 6D). However, knockdown of BAX and BAK expression almost abolished the ability of GX15-070 to promote sorafenib + valproate-induced tumor cell death.

Type II programmed cell death, also called autophagy, is a ubiquitous process that occurs in all eukaryotes. It is morphologically distinct from apoptosis, a different complement of proteins is activated and, unlike apoptosis, may occur under both normal and stressed growth conditions. Autophagy is an apparently nonselective process in which cytoplasm and organelles are randomly assorted into the autophagosome, where they are degraded. The autophagic process is activated by both extracellular (starvation, hormone treat-

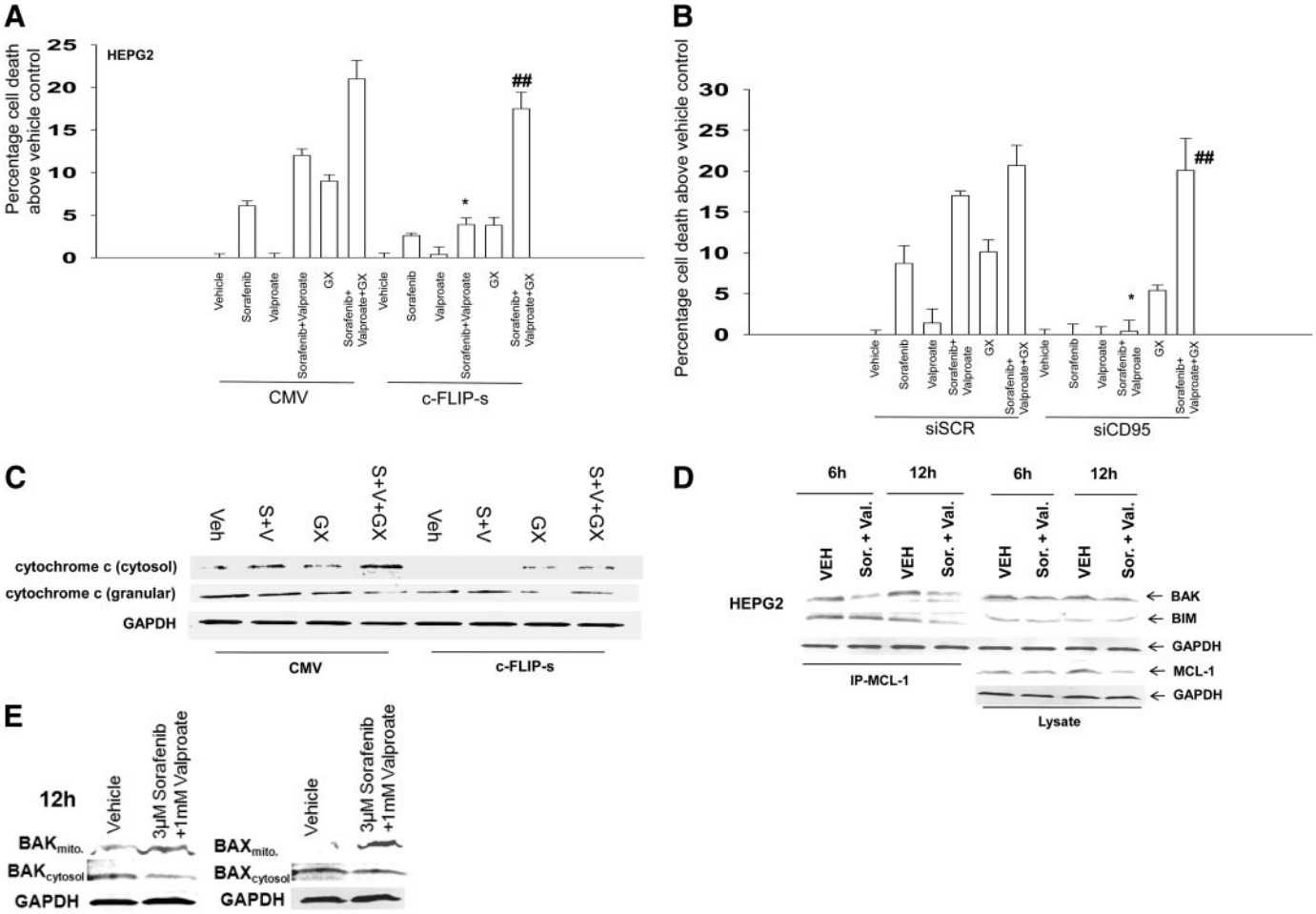

Fig. 5. The BCL-2/BCL-XL/MCL-1 inhibitor GX15-070 promotes sorafenib and valproate-induced killing and circumvents the protective effects of either CD95 knockdown or c-FLIP-s over-expression. A, HEPG2 cells were infected with recombinant adenoviruses, and 24 h after infection, cells were treated with vehicle, sodium valproate, sorafenib, or sorafenib + valproate, and in parallel with either vehicle or GX15-070. Twenty four hours after exposure, cell viability was determined using trypan blue exclusion assays (± S.E.M., $n = 3$). *, $p < 0.05$ less than corresponding value in CMV vector cells; ## $p < 0.05$ greater than cells lacking GX15-070. B, HEPG2 cells were transfected with siRNA to knockdown CD95 (siCD95). Cells were treated 36 h later with vehicle, sodium valproate, sorafenib, or sorafenib + vorinostat and in parallel with either vehicle or GX15-070. Twenty-four hours after drug exposure, viability was determined using trypan blue exclusion (± S.E.M., $n = 3$). *, $p < 0.05$ less than corresponding value in CMV vector cells; ##, $p < 0.05$ greater than cells lacking GX15-070. C, sets of HEPG2 cells parallel to those in A were treated with drugs, and 24 h after exposure, cell fractionation to isolate the crude granular and cytosolic fractions was performed to determine cytochrome *c* levels ($n = 2$). D, HEPG2 cells were treated with vehicle, sodium valproate, sorafenib, or sorafenib + vorinostat, and 12 hours after exposure, equal portions of cell lysate were subjected to immunoprecipitation for MCL-1 or for immunoblotting for total levels of BAK, BIM, and MCL-1 ($n = 2$). E, HEPG2 cells were treated with vehicle, sodium valproate, sorafenib, or sorafenib + vorinostat, and 12 h after exposure, cytosolic and crude granular fractions obtained by differential centrifugation. Equal protein-equal portions of the lysate was subjected to SDS-PAGE followed by immunoblotting to determine the total levels of BAK and BAX in each cell fraction ($n = 2$).

ment, chemotherapy) and intracellular stimuli (e.g., accumulation of unfolded proteins in the ER). Studies from this laboratory have demonstrated that sorafenib + HDACI treatment causes a CD95-dependent form of autophagy, an autophagy that was protective against CD95-induced activation of caspase 8 as judged by knockdown of either ATG5 or Beclin1 (Fig. 7A) (Park et al., 2008a). Knockdown of Beclin1 also suppressed the lethality of GX15-070 as a single agent and the ability of GX15-070 to enhance sorafenib + HDACI-induced killing, regardless of CD95 expression (Fig. 7B). Both sorafenib + HDACI and GX15-070 treatments increased the vesicularization of a transfected LC3 (ATG8)-GFP construct, indicative of autophagy; combined exposure to all three drugs further increased the number of vesicles present in each cell in at least an additive fashion (Fig. 7C). Knockdown of Beclin1 suppressed the ability of all tested drug combinations to increase autophagic vesicle levels. Knockdown of BAX and BAK also suppressed GX15-070 + sorafenib + valproate-induced autophagy (Fig. 7D). Collectively, the data in Figs. 6 and 7 argues that sorafenib + HDACI treatment causes a protective form of autophagy but that exposure to GX15-070, either as a single agent or in combination with that sorafenib + HDACI treatment, promotes tumor cell killing in part by *elevating* levels of a lethal form of autophagy.

Discussion

We have attempted to determine in pancreatic tumor cells whether sorafenib and vorinostat interact synergistically to cause cell death and whether inhibition of mitochondrial BCL-2 family protective protein association with toxic BH3 domain proteins could enhance sorafenib + HDACI lethality in the absence of CD95/death receptor signaling.

The results of the present study indicate that low concentrations of sorafenib and vorinostat interact in a synergistic manner to kill pancreatic cancer cells in vitro. The enhanced lethality of the regimen toward multiple pancreatic cancer cells was also blocked by inhibition of CD95 function and abolished by overexpression of c-FLIP-s. Of particular note, use of a chemically unrelated HDACI, sodium valproate, a widely used generic drug, enhanced the lethality of sorafenib in a fashion nearly identical to that of vorinostat and synergized with sorafenib to kill liver and pancreatic tumor cells. Expression of CD95 enhanced drug-induced cell lethality in hepatoma cells lacking endogenous CD95. Collectively, our present findings argue that pancreatic tumor cells are susceptible to being rapidly killed by sorafenib + HDACI exposure through a death receptor/extrinsic pathway-dependent mechanism.

TABLE 3

GX15-070 restores the synergy of sorafenib + valproate toxicity in cells with blocked extrinsic pathway signaling

Pancreatic cancer (PANC1) cells were infected 12 h after plating at an approximate multiplicity of infection of 50 with either a control empty vector recombinant adenovirus (CMV) or a recombinant virus to express the caspase 8 inhibitor c-FLIP-s. Twenty-four hours after infection, infected cells were plated as single cells (250–1500 cells/well) in sextuplicate; 12 h after this plating, the infected cells were treated with vehicle (DMSO), sorafenib (2.25–3.75 μM), sodium valproate (0.75–1.25 mM), or both drugs combined, as indicated, at a fixed concentration ratio to perform median dose-effect analyses for the determination of synergy. Cells were in parallel treated with either vehicle (DMSO) or GX15-070 (50 nM). After drug exposure (24 h), the medium was changed and cells were cultured in drug-free medium for an additional 10 to 14 days. Cells were fixed and stained with crystal violet, and colonies of >50 cells/colony were counted. Colony formation data were entered into the Calcusyn program, and combination index (CI) values were determined. A CI value of less than 1.00 indicates synergy. Treatment of CMV-infected cells with GX15-070 reduced colony formation as a single agent by 0.63 ± 0.02. Treatment of c-FLIP-s infected cells with GX15-070 reduced colony formation as a single agent by 0.72 ± 0.01.

Treatments	Sorafenib	Valproate	Fa	CI
	μM	mM		
CMV + DMSO	2.25	0.75	0.43	0.72
	3.00	1.00	0.51	0.70
	3.75	1.25	0.66	0.66
CMV + 50 nM GX15-070	2.25	0.75	0.43	0.31
	3.00	1.00	0.51	0.32
	3.75	1.25	0.58	0.26
c-FLIP-s + DMSO	2.25	0.75	0.10	4.55
	3.00	1.00	0.13	3.54
	3.75	1.25	0.19	2.08
c-FLIP-s + 50 nM GX15-070	2.25	0.75	0.43	0.58
	3.00	1.00	0.47	0.5
	3.75	1.25	0.56	0.49

Studies in hepatoma and pancreatic cancer cells treated with sorafenib + vorinostat demonstrated that activated CD95 coimmunoprecipitated with regulators of both apoptosis (e.g., FADD, caspase 8) as well as regulators of ER stress signaling and autophagy (e.g., ATG5, Grp78/BiP). Recent studies from other groups have also argued that CD95/death receptor signaling regulates a protective form of autophagy (Han et al., 2008; Wang et al., 2008). Knockdown of caspase 8 expression can promote a toxic form of autophagy and in some systems, and treatment of cells with the pan-caspase inhibitor *N*-benzyloxycarbonyl-Val-Ala-Asp causes an autophagic form of cell death (Barnhart et al., 2003; Pyo et al., 2005). In our cells, *N*-benzyloxycarbonyl-Val-Ala-Asp did not cause autophagic cell death (M. A. Park and P. Dent, unpublished data). FADD has previously been shown to colocalize with ATG5, and our present data are in agreement with these findings, although in the prior study, interferon-induced FADD-ATG5 signaling in immune cells caused a pro-death autophagy signal (Peták et al., 2001; Barnhart et al., 2003; Park et al., 2005). It is well known that autophagy can promote survival or death based on the cell stressing agent, the cell system being examined, and the cell culture conditions, and the findings in hematopoietic cells with FADD promoting toxic autophagy suggest that in addition to our own data, it is probable that death receptor/FADD/caspase 8/FLIP-regulated autophagy will, under some circumstances, also play a role in toxic forms of autophagy (Han et al., 2008).

An inability to express death receptors or to overexpress dominant-negative–acting forms of death receptors has been linked to apoptosis resistance (Walsh et al., 2003; Park et al., 2005; Dent et al., 2009). HuH7 cells lack CD95 expression and were particularly resistant to sorafenib + HDACI lethality compared with HEPG2 and HEP3B cells that express CD95. Re-expression of CD95 in HuH7 cells facilitated their killing after drug exposure. An additional mechanism that could block toxic death receptor signaling is constitutive high levels of c-FLIP-s. Overexpression of c-FLIP-s protected tumor cells from sorafenib + HDACI-induced tumor cell killing in short- and long-term viability assays. We determined that small-molecule antagonists of BCL-2 family proteins (HA14-1; GX15-070) enhanced sorafenib + HDACI lethality, and in cells overexpressing c-FLIP-s, or where death receptor signaling was suppressed by knockdown of CD95 expression, HA14-1 or obatoclax were capable of reverting sorafenib + HDACI lethality to levels approaching those in vector/siScrambled control cells. Sorafenib + vorinostat treatment activated multiple toxic BH3 domain proteins in cells, includ-

ing BAX, BAK, BID, and BIM, which in the case of BAK was further enhanced in the presence of GX15-070. Thus, promoting a partial activation of the intrinsic apoptosis pathway by use of small molecule antagonists of BCL-2 family protein function; permitted sorafenib + HDACI exposure to cause cell killing independently of death receptor functionality, via the intrinsic pathway.

Prior studies have shown that sorafenib + vorinostat exposure increased the numbers of autophagic vesicles in tumor cells in a CD95- and PERK-dependent fashion and that this form of autophagy was protective against CD95-induced activation of caspase 8/caspase 3 and apoptosis (Park et al., 2008a). The Czaja laboratory recently demonstrated that autophagy induced from death receptor activation is a protective event, whereas autophagy induced from mitochondrial dysfunction is a toxic event (Wang et al., 2008). Others have also shown that death receptor signaling promotes a protective form of autophagy (Han et al., 2008). The BCL-2/BCL-XL inhibitor ABT-737 has been shown to promote autophagy in tumor cells, and we investigated whether the BCL-2/BCL-XL/MCL-1 inhibitor also induced autophagy and whether this played a role in the survival of sorafenib + HDACI-treated cells (Sandoval et al., 2008). Sorafenib + HDACI, GX15-070, and combined exposure to all three drugs increased the vesicularization of a transfected LC3 (ATG8)-GFP construct in a Beclin1- and BAX+BAK-dependent fashion, indicative of autophagy. Knockdown of Beclin1 enhanced the ability of sorafenib + HADCI exposure to kill tumor cells, whereas loss of Beclin1 expression suppressed the ability of GX15-070 as a single agent or when in combination with sorafenib + HDACI to cause cell death. Knockdown of BAX+BAK modestly suppressed sorafenib + HDACI lethal-

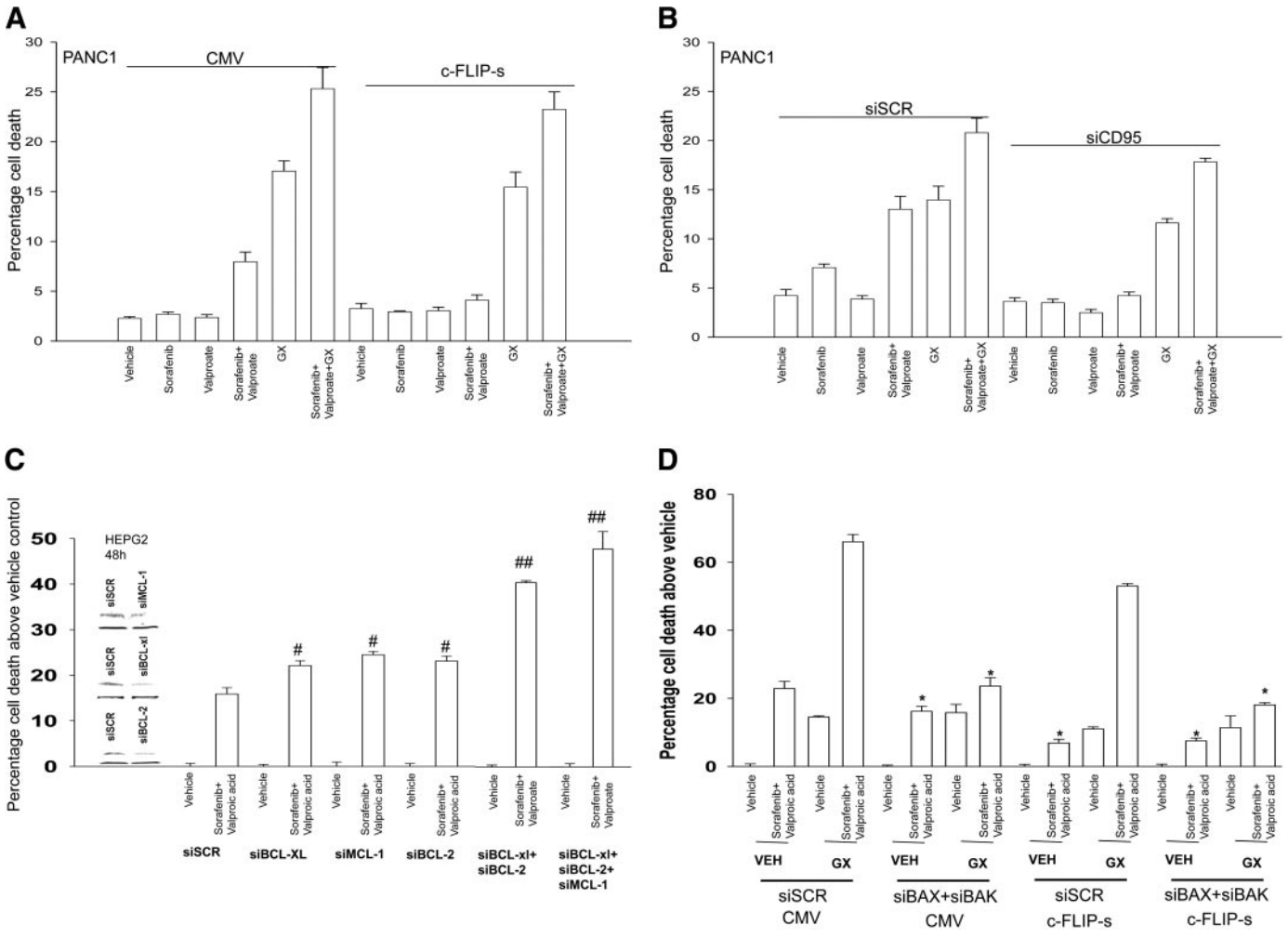

Fig. 6. GX15-070 promotes sorafenib + valproate-induced killing in pancreatic cancer cells. A, PANC1 cells were infected with recombinant adenoviruses, and twenty-four hours after infection, cells were treated with vehicle, sodium valproate, sorafenib, or sorafenib + valproate, in parallel with either vehicle or GX15-070. Twenty-four hours after exposure, cell viability was determined using trypan blue exclusion assays. B, PANC1 cells were transfected with siRNA to knockdown CD95 (siCD95). Thirty-six hours after transfection, cells were treated with vehicle, sodium valproate, sorafenib, or sorafenib + vorinostat and in parallel with either vehicle or GX15-070. Twenty-four hours after exposure, cell viability was determined using a trypan blue exclusion assay (± S.E.M., $n = 3$). C, HEPG2 cells were transfected with scrambled siRNA or transfected with siRNA molecules to knockdown BCL-2, BCL-XL, MCL-1, BCL-2 + BCL-XL, or BCL-2 + BCL-XL + MCL-1 expression. Thirty-six hours after transfection, cells were treated with vehicle, valproate, and sorafenib. Forty-eight hours after exposure, cell viability was determined using a trypan blue exclusion assay (± S.E.M., $n = 4$). #, $p < 0.05$ greater than corresponding value in siSCR cells; ##, $p < 0.05$ greater than cells with single knockdown of a BCL-2 family protein. D, HEPG2 cells were transfected with scrambled siRNA or transfected with siRNA molecules to knockdown BAX and BAK. In parallel, the cells were infected with empty vector virus (CMV) or a virus to express c-FLIP-s. Thirty-six hours after transfection, cells were treated with vehicle, valproate + sorafenib, GX15-070, or GX15-070 + valproate + sorafenib. Forty-eight hours after exposure, cell viability was determined using a trypan blue exclusion assay (± S.E.M., $n = 2$). ∗, $p < 0.05$ less than corresponding value in siSCR cells.

ity but abolished the ability of GX15-070 to restore "two drug" lethality. Thus GX15-070 reverts the apoptosis-resistant phenotype in our CD95 knockdown cell systems through increased toxic autophagy, which requires BAX and BAK function, but in cells that contain a functional extrinsic pathway it does so by simultaneously overwhelming a protective CD95-dependent form of autophagy via a toxic mitochondrial form of autophagy. This data further underscores the essential need for a detailed molecular understanding how any drug combination kills tumor cells.

Sorafenib + HDACI exposure abolished MCL-1 expression within 24 h and reduced expression of BCL-2 and BCL-XL. Knockdown of individual and combinations of BCL-2 family proteins revealed that loss of BCL-2 and BCL-XL expression increased sorafenib + HDACI lethality in a greater than additive manner compared with the summation of individual effects. In contrast, loss of BCL-2, BCL-XL, *and* MCL-1 resulted in a potentiation of killing that was approximately additive between the effects caused by BCL-2 and BCL-XL knockdown and MCL-1 knockdown. Sorafenib as a single agent at higher concentrations induces ER stress signaling with resultant eukaryotic translation initiation factor 2α-dependent translational repression and a lowering in the expression of short-lived proteins such as MCL-1 (Rahmani et al., 2005). Thus a likely reason for our findings with respect to the relative impact of BCL-2 and BCL-XL protein knockdown on sorafenib + HDACI-induced tumor cell killing may be

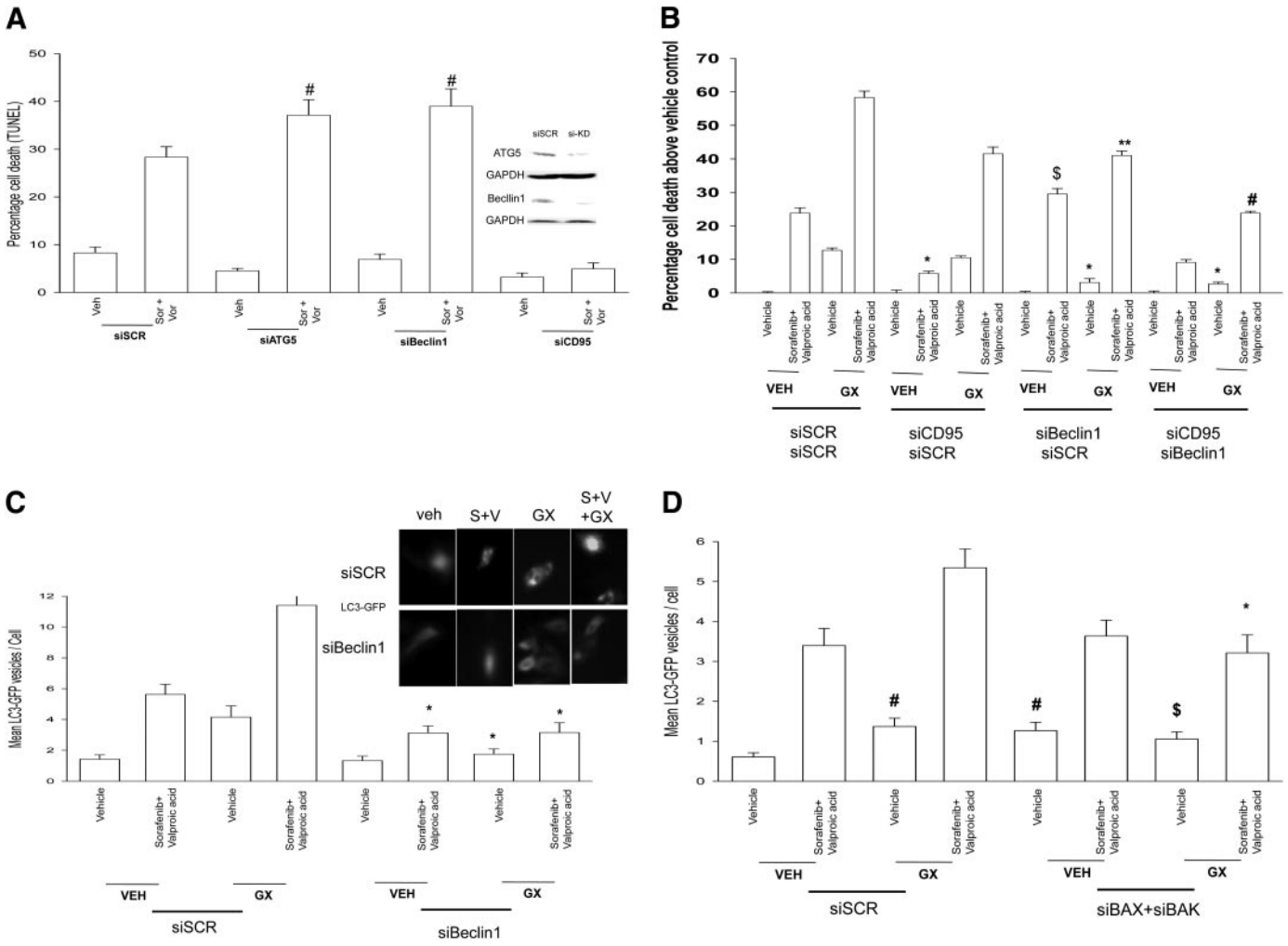

Fig. 7. GX15-070 promotes a toxic form of autophagy to facilitate sorafenib + HDACI killing. A, HEPG2 cells were transfected with scrambled siRNA (siSCR) or transfected with siRNA molecules to knockdown expression of ATG5, Beclin1, or CD95. Thirty-six hours after transfection, cells were treated with vehicle, vorinostat, and sorafenib. Forty-eight hours after exposure, cell viability was determined using a trypan blue exclusion assay ($\pm$ S.E.M., $n = 2$). #, $p < 0.05$ greater than corresponding value in siSCR cells. B, HEPG2 cells were transfected with siSCR or transfected with siRNA molecules to knockdown expression of Beclin1 and/or CD95. Thirty-six hours after transfection, cells were treated with vehicle, GX15-070, valproate, and sorafenib. Forty-eight hours after exposure, cell viability was determined using a trypan blue exclusion assay ($\pm$ S.E.M., $n = 2$). $*$, $p < 0.05$ less than corresponding value in siSCR cells; \$, $p < 0.05$ greater than corresponding value in siSCR cells; #, $p < 0.05$ less than corresponding value in siBeclin1 cells; $**$, $p > 0.05$ the corresponding value in siCD95 cells. C, HEPG2 cells were transfected with a plasmid to express LC3-GFP and in parallel were transfected with scrambled siRNA (siSCR) or transfected with siRNA molecules to knockdown expression of Beclin1. Thirty-six hours after transfection, cells were treated with vehicle, GX15-070, valproate, and sorafenib. Six hours after exposure, the vesicularization of the LC3-GFP construct was determined using fluorescent microscopy ($\pm$ S.E.M., $n = 2$). $*$, $p < 0.05$ less than corresponding value in siSCR cells. D, HEPG2 cells were transfected with a plasmid to express LC3-GFP and in parallel were transfected with siSCR or transfected with siRNA molecules to knockdown expression of BAX and BAK. Thirty-six hours after transfection, cells were treated with vehicle, GX15-070, valproate, and sorafenib. Six hours after exposure, the vesicularization of the LC3-GFP construct was determined using fluorescent microscopy ($\pm$ S.E.M., $n = 2$). $*$, $p < 0.05$ less than corresponding value in siSCR cells.

due to the greater reduction of short-lived MCL-1 expression caused by sorafenib + HDACI exposure.

Sorafenib + HDACI exposure leads to CD95/caspase 8 activation, causing BID cleavage. Cleaved BID as a BH3-only domain protein can act to displace BAX, BAK, and BIM from protective BCL-2 family proteins, resulting in homo-oligomerization of BAK and possible association with BAX, resulting in mitochondrial pore formation and release of cytochrome *c* into the cytosol. The finding that GX15-070 as a single agent induced conformational change in BAX (and to a lesser extent BAK), but only weakly triggered apoptosis by itself, suggests that the lethality of the (sorafenib + HDACI) + GX15-070 regimen involves not simply activation of either BAX or BAK, but a cooperative interaction between these proteins together with the loss of protective BCL-2 family protein levels. The notion of cooperative BAX and BAK actions in the regulation of sorafenib + HDACI lethality is further supported by the results obtained in BAX(−/−), BAK(−/−), and BAX-BAK(−/−) transformed MEFs, as well as using siRNA knockdown of BAX + BAK in hepatoma cells. BAX(−/−) MEFs were more resistant to sorafenib + HDACI lethality than BAK(−/−) cells; however, deletion of both proteins abolished drug lethality in MEFs, and siRNA knockdown partially reduced sorafenib + HDACI lethality in hepatoma cells. Because sorafenib + vorinostat therapy is about to be explored in a phase I trial in hepatoma, our data suggest that the incorporation of GX15-070 (obatoclax) together with sorafenib + HDACI therapy, may provide significant additional value in tumor control, including tumors that lack extrinsic pathway signaling.

In conclusion, the results of the present study indicate that sorafenib and multiple HDACIs interact in a highly synergistic manner to kill pancreatic tumor cells in vitro via activation of CD95. These effects are magnified when BCL-2 family protein activity is inhibited and demonstrate for the first time that loss of extrinsic pathway activation that blocks cell killing is circumvented by use of a small molecule BCL-2 inhibitor, which restores drug-induced cell killing in part through toxic autophagy. Ongoing in vitro and future animal studies will be required to fully define the importance of sorafenib and vorinostat (or other HDACIs) as a therapeutic in cancer.

References

Allan LA, Morrice N, Brady S, Magee G, Pathak S, and Clarke PR (2003) Inhibition of caspase-9 through phosphorylation at Thr 125 by ERK MAPK. *Nat Cell Biol* **5:**647–654.

Azmi AS and Mohammad RM (2009) Non-peptidic small molecule inhibitors against Bcl-2 for cancer therapy. *J Cell Physiol* **218:**13–21.

Bali P, Pranpat M, Swaby R, Fiskus W, Yamaguchi H, Balasis M, Rocha K, Wang HG, Richon V, and Bhalla K (2005) Activity of suberoylanilide hydroxamic Acid against human breast cancer cells with amplification of her-2. *Clin Cancer Res* **11:**6382–6389.

Bardeesy N and DePinho RA (2002) Pancreatic cancer biology and genetics. *Nat Rev Cancer* **2:**897–909.

Barnhart BC, Alappat EC, and Peter ME (2003) The CD95 type I/type II model. *Semin Immunol* **15:**185–193.

Chen S, Dai Y, Harada H, Dent P, and Grant S (2007) Mcl-1 down-regulation potentiates ABT-737 lethality by cooperatively inducing Bak activation and Bax translocation. *Cancer Res* **67:**782–791.

Dai Y and Grant S (2007) Targeting multiple arms of the apoptotic regulatory machinery. *Cancer Res* **67:**2908–2911.

Dasmahapatra G, Yerram N, Dai Y, Dent P, and Grant S (2007) Synergistic interactions between vorinostat and sorafenib in chronic myelogenous leukemia cells involve Mcl-1 and p21CIP1 down-regulation. *Clin Cancer Res* **13:**4280–4290.

Davies BR, Logie A, McKay JS, Martin P, Steele S, Jenkins R, Cockerill M, Cartlidge S, and Smith PD (2007) AZD6244 (ARRY-142886), a potent inhibitor of mitogen-activated protein kinase/extracellular signal-regulated kinase kinase 1/2 kinases: mechanism of action in vivo, pharmacokinetic/pharmacodynamic relationship, and potential for combination in preclinical models. *Mol Cancer Ther* **6:**2209–2219.

Dent P, Yacoub A, Fisher PB, Hagan MP, and Grant S (2003) MAPK pathways in radiation responses. *Oncogene* **22:**5885–5896.

Dent P (2005) MAP kinase pathways in the control of hepatocyte growth, metabolism and survival, in *Signaling Pathways in Liver Diseases* (DuFour JF, Clavien PA eds) pp 223–238, Springer, New York.

Dent P, Curiel DT, Fisher PB, and Grant S (2009) Synergistic combinations of signaling pathway inhibitors: Mechanisms for improved cancer therapy. *Drug Resist Updat* doi:10.1016/j.drup.2009.03.001

Flaherty KT (2007) Sorafenib: delivering a targeted drug to the right targets. *Expert Rev Anticancer Ther* **7:**617–626.

Gollob JA (2005) Sorafenib: scientific rationales for single-agent and combination therapy in clear-cell renal cell carcinoma. *Clin Genitourin Cancer* **4:**167–174.

Grant S and Dent P (2004) Kinase inhibitors and cytotoxic drug resistance. *Clin Cancer Res* **10:**2205–2207.

Gregory PD, Wagner K, and Hörz W (2001) Histone acetylation and chromatin remodeling. *Exp Cell Res* **265:**195–202.

Han J, Hou W, Goldstein LA, Lu C, Stolz DB, Yin XM, and Rabinowich H (2008) Involvement of protective autophagy in TRAIL resistance of apoptosis-defective tumor cells. *J Biol Chem* **283:**19665–19677.

Kang MH and Reynolds CP (2009) Bcl-2 inhibitors: targeting mitochondrial apoptotic pathways in cancer therapy. *Clin Cancer Res* **15:**1126–1132.

Konopleva M, Watt J, Contractor R, Tsao T, Harris D, Estrov Z, Bornmann W, Kantarjian H, Viallet J, Samudio I, et al. (2008) Mechanisms of antileukemic activity of the novel Bcl-2 homology domain-3 mimetic GX15-070 (obatoclax). *Cancer Res* **68:**3413–3420.

Kwon SH, Ahn SH, Kim YK, Bae GU, Yoon JW, Hong S, Lee HY, Lee YW, Lee HW, and Han JW (2002) Apicidin, a histone deacetylase inhibitor, induces apoptosis and Fas/Fas ligand expression in human acute promyelocytic leukemia cells. *J Biol Chem* **277:**2073–2080.

Lessene G, Czabotar PE, and Colman PM (2008) BCL-2 family antagonists for cancer therapy. *Nat Rev Drug Discov* **7:**989–1000.

Ley R, Balmanno K, Hadfield K, Weston C, and Cook SJ (2003) Activation of the ERK1/2 signaling pathway promotes phosphorylation and proteasome-dependent degradation of the BH3-only protein, Bim. *J Biol Chem* **278:**18811–18816.

Li N, Batt D, and Warmuth M (2007) B-Raf kinase inhibitors for cancer treatment. *Curr Opin Investig Drugs* **8:**452–456.

Marks PA, Miller T, and Richon VM (2003) Histone deacetylases. *Curr Opin Pharmacol* **3:**344–351.

Mitchell C, Park MA, Zhang G, Han SI, Harada H, Franklin RA, Yacoub A, Li PL, Hylemon PB, Grant S, et al. (2007) 17-Allylamino-17-demethoxygeldanamycin enhances the lethality of deoxycholic acid in primary rodent hepatocytes and established cell lines. *Mol Cancer Ther* **6:**618–632.

Mori M, Uchida M, Watanabe T, Kirito K, Hatake K, Ozawa K, and Komatsu N (2003) Activation of extracellular signal-regulated kinases ERK1 and ERK2 induces Bcl-xL up-regulation via inhibition of caspase activities in erythropoietin signaling. *J Cell Physiol* **195:**290–297.

Nguyen M, Marcellus RC, Roulston A, Watson M, Serfass L, Murthy Madiraju SR, Goulet D, Viallet J, Bélec L, Billot X, et al. (2007) Small molecule obatoclax (GX15-070) antagonizes MCL-1 and overcomes MCL-1-mediated resistance to apoptosis. *Proc Natl Acad Sci U S A* **104:**19512–19517.

Oltersdorf T, Elmore SW, Shoemaker AR, Armstrong RC, Augeri DJ, Belli BA, Bruncko M, Deckwerth TL, Dinges J, Hajduk PJ, et al. (2005) An inhibitor of Bcl-2 family proteins induces regression of solid tumours. *Nature* **435:**677–681.

Pang RW and Poon RT (2007) From molecular biology to targeted therapies for hepatocellular carcinoma: the future is now. *Oncology* **72 (Suppl 1):**30–44.

Park MA, Zhang G, Martin AP, Hamed H, Mitchell C, Hylemon PB, Graf M, Rahmani M, Ryan K, Liu X, et al. (2008a) Vorinostat and sorafenib increase ER stress, autophagy and apoptosis via ceramide-dependent CD95 and PERK activation. *Cancer Biol Ther* **7:**1648–1662.

Park MA, Yacoub A, Rahmani M, Zhang G, Hart L, Hagan MP, Calderwood SK, Sherman MY, Koumenis C, Spiegel S, et al. (2008b) OSU-03012 stimulates PKR-like endoplasmic reticulum-dependent increases in 70-kDa heat shock protein expression, attenuating its lethal actions in transformed cells. *Mol Pharmacol* **73:**1168–1184.

Park MA, Zhang G, Mitchell C, Rahmani M, Hamed H, Hagan MP, Yacoub A, Curiel DT, Fisher PB, Grant S, et al. (2008c) Mitogen-activated protein kinase kinase 1/2 inhibitors and 17-allylamino-17-demethoxygeldanamycin synergize to kill human gastrointestinal tumor cells in vitro via suppression of c-FLIP-s levels and activation of CD95. *Mol Cancer Ther* **7:**2633–2648.

Park SM, Schickel R, and Peter ME (2005) Nonapoptotic functions of FADD-binding death receptors and their signaling molecules. *Curr Opin Cell Biol* **17:**610–616.

Parkin DM, Bray F, Ferlay J, and Pisani P (2005) Global cancer statistics, 2002. *CA Cancer J Clin* **55:**74–108.

Peták I and Houghton JA (2001) Shared pathways: death receptors and cytotoxic drugs in cancer therapy. *Pathol Oncol Res* **7:**95–106.

Pyo JO, Jang MH, Kwon YK, Lee HJ, Jun JI, Woo HN, Cho DH, Choi B, Lee H, Kim JH, et al. (2005) Essential roles of Atg5 and FADD in autophagic cell death: dissection of autophagic cell death into vacuole formation and cell death. *J Biol Chem* **280:**20722–20729.

Qiao L, Studer E, Leach K, McKinstry R, Gupta S, Decker R, Kukreja R, Valerie K, Nagarkatti P, El Deiry W, et al. (2001) Deoxycholic acid (DCA) causes ligand-independent activation of epidermal growth factor receptor (EGFR) and FAS receptor in primary hepatocytes: inhibition of EGFR/mitogen-activated protein kinase-signaling module enhances DCA-induced apoptosis. *Mol Biol Cell* **12:**2629–2645.

Qiao L, Han SI, Fang Y, Park JS, Gupta S, Gilfor D, Amorino G, Valerie K, Sealy L, Engelhardt JF, et al. (2003) Bile acid regulation of C/EBPbeta, CREB, and c-Jun function, via the extracellular signal-regulated kinase and c-Jun NH2-terminal kinase pathways, modulates the apoptotic response of hepatocytes. *Mol Cell Biol* **23:**3052–3066.

Rahmani M, Davis EM, Bauer C, Dent P, and Grant S (2005) Apoptosis induced by the kinase inhibitor BAY 43–9006 in human leukemia cells involves down-regulation of Mcl-1 through inhibition of translation. *J Biol Chem* **280:**35217–35227.

Rahmani M, Nguyen TK, Dent P, and Grant S (2007a) The multikinase inhibitor sorafenib induces apoptosis in highly imatinib mesylate-resistant bcr/abl+ human leukemia cells in association with signal transducer and activator of transcription 5 inhibition and myeloid cell leukemia-1 down-regulation. *Mol Pharmacol* **72:**788–795.

Rahmani M, Davis EM, Crabtree TR, Habibi JR, Nguyen TK, Dent P, and Grant S (2007b) The kinase inhibitor sorafenib induces cell death through a process involving induction of endoplasmic reticulum stress. *Mol Cell Biol* **27:**5499–5513.

Rini BI (2006) Sorafenib. *Expert Opin Pharmacother* **7:**453–461.

Rodriguez-Menendez V, Tremolizzo L, and Cavaletti G (2008) Targeting cancer and neuropathy with histone deacetylase inhibitors: two birds with one stone? *Curr Cancer Drug Targets* **8:**266–274.

Sandoval H, Thiagarajan P, Dasgupta SK, Schumacher A, Prchal JT, Chen M, and Wang J (2008) Essential role for Nix in autophagic maturation of erythroid cells. *Nature* **454:**232–235.

Strumberg D (2005) Preclinical and clinical development of the oral multikinase inhibitor sorafenib in cancer treatment. *Drugs Today* (*Barc*) **41:**773–784.

Susnow N, Zeng L, Margineantu D, and Hockenbery DM (2009) Bcl-2 family proteins as regulators of oxidative stress. *Semin Cancer Biol* **19:**42–49.

Valerie K, Yacoub A, Hagan MP, Curiel DT, Fisher PB, Grant S, and Dent P (2007) Radiation-induced cell signaling: inside-out and outside-in. *Mol Cancer Ther* **6:**789–801.

Venturelli S, Armeanu S, Pathil A, Hsieh CJ, Weiss TS, Vonthein R, Wehrmann M, Gregor M, Lauer UM, and Bitzer M (2007) Epigenetic combination therapy as a tumor-selective treatment approach for hepatocellular carcinoma. *Cancer* **109:**2132–2141.

Walsh CM, Luhrs KA, and Arechiga AF (2003) The "fuzzy logic" of the death-inducing signaling complex in lymphocytes. *J Clin Immunol* **23:**333–353.

Wang Y, Singh R, Massey AC, Kane SS, Kaushik S, Grant T, Xiang Y, Cuervo AM, and Czaja MJ (2008) Loss of macroautophagy promotes or prevents fibroblast apoptosis depending on the death stimulus. *J Biol Chem* **283:**4766–4777.

Wang YF, Jiang CC, Kiejda KA, Gillespie S, Zhang XD, and Hersey P (2007) Apoptosis induction in human melanoma cells by inhibition of MEK is caspase-independent and mediated by the Bcl-2 family members PUMA, Bim, and Mcl-1. *Clin Cancer Res* **13:**4934–4942.

Wise LD, Turner KJ, and Kerr JS (2007) Assessment of developmental toxicity of vorinostat, a histone deacetylase inhibitor, in Sprague-Dawley rats and Dutch Belted rabbits. *Birth Defects Res B Dev Reprod Toxicol* **80:**57–68.

Yacoub A, Park MA, Gupta P, Rahmani M, Zhang G, Hamed H, Hanna D, Sarkar D, Lebedeva IV, Emdad L, et al. (2008) Caspase-, cathepsin-, and PERK-dependent regulation of MDA-7/IL-24-induced cell killing in primary human glioma cells. *Mol Cancer Ther* **7:**297–313.

Zhang G, Park MA, Mitchell C, Hamed H, Rahmani M, Martin AP, Curiel DT, Yacoub A, Graf M, Lee R, et al. (2008) Vorinostat and sorafenib synergistically kill tumor cells via FLIP suppression and CD95 activation. *Clin Cancer Res* **14:**5385–5399.

Zhang L, Ming L, and Yu J (2007) BH3 mimetics to improve cancer therapy; mechanisms and examples. *Drug Resist Updat* **10:**207–217.

Address correspondence to: Dr. Paul Dent, Department of Biochemistry and Molecular Biology, 401 College Street, Massey Cancer Center, Room 280a, Box 980035, Virginia Commonwealth University, Richmond VA 23298-0035. E-mail: pdent@vcu.edu